nature chemical biology

BRIEF COMMUNICATION

PUBLISHED ONLINE: 6 DECEMBER 2013 | DOI: 10.1038/NCHEMBIO.1432

A METTL3–METTL14 complex mediates mammalian nuclear RNA N^6-adenosine methylation

Jianzhao Liu[1–3], Yanan Yue[1–3], Dali Han[1,2], Xiao Wang[1,2], Ye Fu[1,2], Liang Zhang[1,2], Guifang Jia[1,2], Miao Yu[1,2], Zhike Lu[1,2], Xin Deng[1,2], Qing Dai[1,2], Weizhong Chen[1,2] & Chuan He[1,2]*

N^6-methyladenosine (m^6A) is the most prevalent and reversible internal modification in mammalian messenger and noncoding RNAs. We report here that human methyltransferase-like 14 (METTL14) catalyzes m^6A RNA methylation. Together with METTL3, the only previously known m^6A methyltransferase, these two proteins form a stable heterodimer core complex of METTL3–METTL14 that functions in cellular m^6A deposition on mammalian nuclear RNAs. WTAP, a mammalian splicing factor, can interact with this complex and affect this methylation.

m^6A is a conserved internal modification found in almost all eukaryotic nuclear RNAs[1–3] as well as in the viral RNA that replicates inside host nuclei[4]. The discoveries of functionally important demethylases that reverse this methylation[5,6], together with the recently revealed m^6A distributions in mammalian transcriptomes[7,8], strongly indicate regulatory functions of this dynamic modification.

The m^6A modification is post-transcriptionally installed by a multicomponent N^6-adenosine methyltransferase (MT) complex yet to be fully identified and characterized. From a ~200-kDa MT complex isolated from mammalian cell nuclear extract that exhibits methyltransferase activity, only a 70-kDa protein was identified, and it was named MT-A70 (or METTL3)[9]. Knockdown of METTL3 led to apoptosis of human HeLa cells[1], whereas the deficiency of its homologs in other species resulted in developmental arrest or defects in gametogenesis[10–12].

In mammals, mRNA methylation occurs within a consensus sequence of Pu(G>A)m^6AC(A/C/U) (where Pu represents purine), though only a portion of these putative methylation sites contain m^6A (ref. 7). How the methylation pattern and methylation level on mRNA are regulated *in vivo* is unclear largely because the methyltransferase complex itself has not yet been revealed. A phylogenetic analysis of the MT-A70 family of methyltransferases suggested that METTL14, which shares 43% identity with METTL3 (**Supplementary Results, Supplementary Note 1**), is a homolog of METTL3 (ref. 13). METTL3 and METTL14 are highly conserved in mammals (**Supplementary Notes 2** and **3**), a feature that prompted us to ask whether METTL14 contributes to mRNA methylation in mammalian cells. Meanwhile, recent studies in *Arabidopsis* and yeast suggested that homologs of a mammalian pre-mRNA splicing regulator, WTAP[14], are involved in RNA methylation[12,15]. We therefore also included WTAP in our investigation.

We knocked down METTL3, METTL14 and WTAP to check the m^6A levels in HeLa and 293FT cells using siRNAs (over 80% knockdown after 48 h; **Supplementary Fig. 1** and **Supplementary Table 1**). The LC/MS/MS results indicated that knockdown of cellular METTL3, METTL14 and WTAP decreased m^6A in polyadenylated RNA by ~30%, ~40% and ~50% in HeLa cells, respectively, and by ~20%, ~35% and ~42% in 293FT cells, respectively (**Fig. 1a** and **Supplementary Fig. 2**). Both METTL14 and WTAP have a larger effect on m^6A level than METTL3. In contrast, when we knocked down METTL4 (close to 80% knockdown efficiency), a close mammalian homolog of METTL3 and METTL14, we did not observe any noticeable change in m^6A level in the isolated polyadenylated RNA (**Supplementary Fig. 1a**).

We expressed the recombinant proteins of METTL3, METTL14 and WTAP from insect cells (with different tags, including Flag, GST and His_6) for biochemical characterizations (**Supplementary Fig. 3a**). Each Flag-tagged protein was purified by anti-Flag resins and subjected to gel filtration analysis. METTL3 and METTL14 form a stable METTL3–METTL14 complex in the gel filtration experiment (**Fig. 1b** and **Supplementary Fig. 3b,c**). Subsequent two-dimensional native–SDS PAGE analysis of the co-expressed METTL3 and METTL14 further confirmed formation of a complex between these two proteins with a stoichiometry of 1:1 (**Fig. 1c** and **Supplementary Fig. 3d**). WTAP appears to form aggregates, as revealed by its much larger apparent molecular weight, calculated from the gel filtration trace (**Fig. 1b**). WTAP can bind the METTL3–METTL14 complex; however, a much lower stoichiometry of WTAP to METTL3 or METTL14 was observed in the co-immunoprecipitation (co-IP) experiment (**Supplementary Fig. 3a**), indicating a relatively weaker interaction between WTAP and these two methyltransferases.

To study the cellular interactions among these proteins, we expressed Flag-tagged METTL3, METTL14 or WTAP in HeLa cells and pulled them down using anti-Flag beads. Western blotting, silver staining and MS protein identification were used to characterize the protein components in each IP fraction (**Supplementary Fig. 4a** and **Supplementary Tables 4–9**). Indeed, the pulldown in each IP experiment contained the other two proteins. Close examination of the cell extract input, IP and flow-through (FT) fractions by western blotting led us to conclude that METTL3 and METTL14 exist as a stable complex inside cells (**Supplementary Fig. 4b**). Consistent with the *in vitro* observation, the interactions between WTAP and the two methyltransferases are weaker. As a control, none of the IP products contained the homologous methyltransferase METTL4 (**Supplementary Fig. 4c**).

Next, we tested N^6-adenosine methylation activity for each recombinant protein and the combination of METTL3 and METTL14 toward various synthetic RNA probes (**Fig. 2** and **Supplementary Fig. 5**). *S*-(5′-Adenosyl)-L-methionine-d_3 (d_3-SAM; **1**), with a deuterium-substituted methyl group, was used as the cofactor for accurate MS quantification. We calculated the molar ratio of the formed d_3-m^6A (**2**) to each

[1]Department of Chemistry, University of Chicago, Chicago, Illinois, USA. [2]Institute for Biophysical Dynamics, University of Chicago, Chicago, Illinois, USA. [3]These authors contributed equally to this work.
*e-mail: chuanhe@uchicago.edu

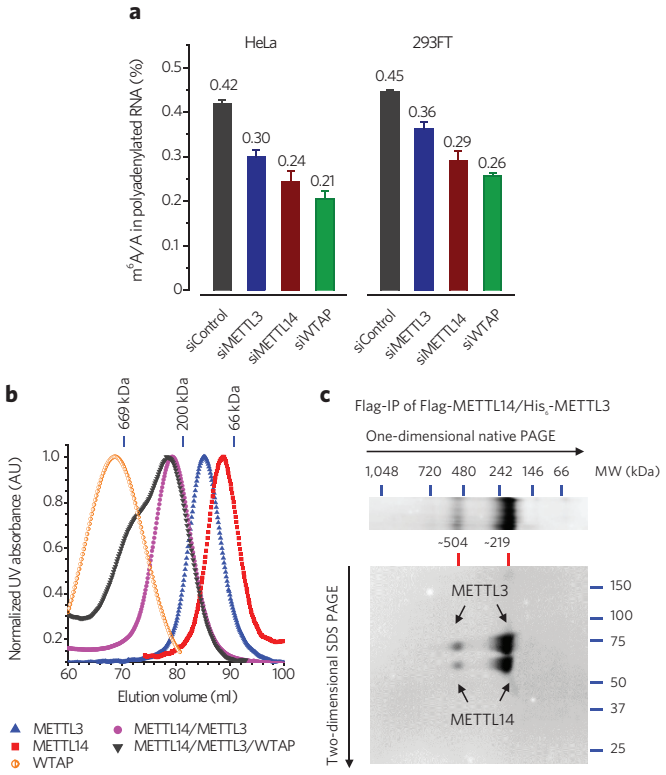

Figure 1 | METTL3, METTL14 and WTAP affect the cellular m^{6}A level in polyadenylated RNA with METTL3 and METTL14 forming a stable complex. (**a**) LC/MS/MS quantification of the m^{6}A/A ratio in polyadenylated RNA isolated from HeLa and 293FT cells with the control and single knockdown of METTL3, METTL14 or WTAP. Both groups of data were assessed using Student's *t*-test with $P < 1 \times 10^{-6}$ (relative to control). Error bars indicate mean ± s.d. ($n = 10$ for HeLa, five biological replicates × two technical replicates; $n = 8$ for 293FT, four biological replicates × two technical replicates). (**b**) Gel filtration traces of individual Flag-tagged METTL3, METTL14 and WTAP; co-expressed Flag-METTL14 and His$_6$-METTL3; and mixed Flag-METTL14, Flag-METTL3 and Flag-WTAP with equal molar amounts. All proteins were expressed in insect cells and purified by Flag-IP. Markers: 669 kDa (thyroglobulin, bovine), 200 kDa (β-amylase from sweet potato) and 66 kDa (BSA). (**c**) Coomassie blue staining of two-dimensional native/SDS PAGE of the Flag-IP product from insect cells coexpressing Flag-METTL14 and His$_6$-METTL3. The band at ~219 kDa corresponds to the METTL3–METTL14 heterodimer, and the band at ~504 kDa represents the dimer of dimer. Full images of gels are presented in **Supplementary Figure 15**. MW, molecular weight.

RNA probe to quantify the methylation efficiency. As RNA probe 1 has two consensus motifs located in both stem and loop, the theoretical maximum value for d_3-m^{6}A/probe is 2. All other probes have a d_3-m^{6}A/probe maxima of 1.

WTAP itself showed no methyltransferase activity with all probes tested, whereas both METTL3 and METTL14 had methyltransferase activity, with METTL14 showing much higher activity (close to tenfold with several probes) than METTL3 (**Fig. 2**). For instance, when RNA probe 1 was tested, Flag-tagged METTL14 afforded a d_3-m^{6}A/probe value of 0.24 compared to 0.02, which was observed for METTL3 under the same conditions. Furthermore, the METTL3-METTL14 combination (~1.04, d_3-m^{6}A/probe) markedly enhances methyltransferase activity compared to each individual protein, demonstrating a synergistic effect. The same reactivity trend was also observed for other probes containing the consensus sequence. In addition, when we combined the cellular IP products of METTL3 and METTL14 and compared the methylation activity with that of the each individual IP fraction, the same synergistic effect was observed (**Supplementary Fig. 4d**).

Both METTL3 and METTL14 preferentially methylate RNA substrates containing the previously revealed consensus sequence. When RNA probes 1 and 5 (containing a GGACU motif) were used, ~11- to 64-fold higher methylation efficiency was observed relative to the same experiments conducted using RNA probes 4 and 6, which have a change of C to U (GGAUU) in the consensus sequence (**Fig. 2**). We further synthesized RNA probes 2 and 3 with only one GGACU sequence in the loop and stem, respectively. The METTL3-METTL14 combination exhibited slightly higher activity toward probe 3 (GGACU in the stem) than probe 2 (GGACU in the loop). As very little activity was observed for probe 4, our results confirm that GGACU is required for optimal activity either in the loop or stem. Additionally, the METTL3–METTL14 combination showed very high activity to probe 5 with a random structure, indicating no obvious preference of these methyltransferases to the RNA secondary structure for m^{6}A deposition. These results indicate that these methyltransferases have sequence specificity but show less structural preference to RNA substrates.

We next isolated the native HeLa cell nuclear extract (NE) according to the published procedure (**Supplementary Fig. 6a**)[16] and tested the methylation activity of each NE fraction at each separation step (**Supplementary Fig. 6b**). As a result, the NE fractions A2-19 to A2-21, which exhibited the highest activity, were found to be enriched with METTL3 and METTL14 (**Supplementary Fig. 6b**). These three fractions were combined. Western blotting of native PAGE gel of the combined fractions showed that both METTL3 and METTL14 migrate to the same front, marked with an apparent molecular weight of ~240 kDa, indicating their presence in a heterodimer complex (**Supplementary Fig. 6c**). Indirect immunofluorescence analysis in HeLa cells clearly demonstrated that METTL3, METTL14 and WTAP localize well with each other (Pearson correlation coefficient = 0.83-0.91) in well-defined, irregular dot-like structures inside the nucleus, with no fluorescence signal observed in the cytoplasm (**Supplementary Fig. 7**).

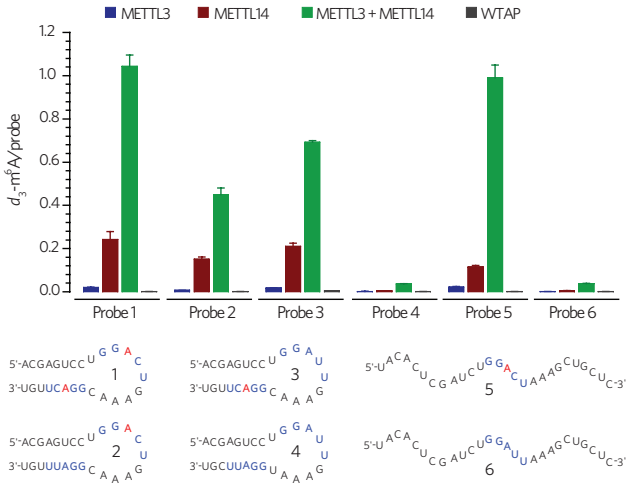

Figure 2 | *In vitro* methylation activity of METTL3, METTL14 and WTAP. The *in vitro* RNA *N*^{6}-adenosine methylation activities of Flag-tagged METTL3, METTL14 or WTAP as well as the combination of METTL3 and METTL14 were tested using different RNA probes (numbered 1–6) with or without the consensus sequence of GGACU in the stem and/or loop and with or without a stem-loop secondary structure in the presence of isotope-labeled cofactor d_3-SAM. The methylation yields were calculated on the basis of the molar ratio of d_3-m^{6}A to specific probe, measured by LC/MS/MS. Error bars indicate mean ± s.d., $n = 4$ (two biological replicates × two technical replicates).

We also found that these three proteins all localize well together with various pre-mRNA processing factors residing in the nuclear speckles (**Supplementary Fig. 8**). Taken together, we concluded that METTL3 and METTL14 can form a stable complex to perform the m^{6}A methylation function inside mammalian cells. WTAP can interact with this complex to affect cellular m^{6}A deposition.

We further performed photoactivatable ribonucleoside-enhanced crosslinking and immunoprecipitation (PAR-CLIP)[17] with 4-thiouridine (4SU)-treated HeLa cells to identify the direct binding sites of these proteins. The crosslinked RNA segments were isolated, converted into cDNA libraries and subjected to high-throughput sequencing. Analyses of sequenced clusters yielded the enriched binding motifs of GGAC for METTL14 and METTL3 and GACU for WTAP (**Fig. 3a** and **Supplementary Fig. 9a**), all of which are consistent with the previously identified consensus sequence of Pu(G>A)m^{6}AC(A/C/U) for m^{6}A. METTL14 and METTL3 have an average of ~56% binding sites in common, whereas all three proteins have ~36% common binding sites (**Supplementary Fig. 9b**).

Our subsequent analyses revealed that a large fraction of the binding sites for all three proteins fall into intergenic regions (~43–49%) and introns (~29-34%) (**Supplementary Fig. 9c** and **Supplementary Data Sets 1–3**). The binding sites that could be assigned to genes are mainly located in the coding sequence and the 3′ UTR (**Supplementary Fig. 9d**), consistent with the peak distribution of m^{6}A in mammalian nuclear RNA[7,8]. METTL3 (2,110 genes) and METTL14 (1,147 genes) share an average of ~57% common target genes (**Supplementary Fig. 9e**). Notably, 261 of the METTL3 target genes are enriched in the functional pathways related to 'cell death and cellular response to stress' (**Supplementary Fig. 10**). Consistent with the previous report[1], the viability of HeLa cells was markedly reduced after 72-h knockdown of METTL3. The knockdown of the other two proteins also led to cell death (**Supplementary Fig. 11**).

The PAR-CLIP sites were compared to the transcriptome-wide m^{6}A distribution obtained in the same cell line. The target genes of the three proteins identified by PAR-CLIP have ~50% overlap with the m^{6}A-containing genes (**Supplementary Fig. 12**). Meanwhile, we found that silencing of METTL3, METTL14 or WTAP led to noticeable increases (~15-26%) of the abundance of their m^{6}A target transcripts compared to that of all transcripts (**Supplementary Fig. 13** and **Supplementary Data Sets 4–6**). We further revealed that reduced global m^{6}A methylation increases the lifetime of nascent RNAs (**Supplementary Fig. 14**). Together, these results indicate an overall negative impact on gene expression by installing m^{6}A on mRNA, consistent with an m^{6}A-dependent mRNA degradation process as one main function of the m^{6}A methylation[18].

In summary, we discovered a new methyltransferase, METTL14, that forms a stable heterodimer with METTL3. This METTL3–METTL14 complex mediates m^{6}A deposition on nuclear RNA inside mammalian cells. WTAP does not have methylation activity, but it interacts with the METTL3–METTL14 complex to markedly affect cellular m^{6}A deposition. The METTL3–METTL14 complex and the recently discovered m^{6}A RNA demethylases could dynamically regulate m^{6}A in mRNA and other nuclear RNA through opposing enzymatic functions (**Fig. 3b**). Contributions from each component to the methylation and their impacts on different biological pathways need to be carefully investigated. By characterizing the methyltransferase core complex, this study provides the basis for these future mechanistic investigations of biological functions associated with m^{6}A deposition[1,2,5–8,19].

METHODS

Methods and any associated references are available in the online version of the paper.

Accession codes. Gene Expression Omnibus. The PAR-CLIP and m^{6}A-seq data were deposited under accession number GSE46705.

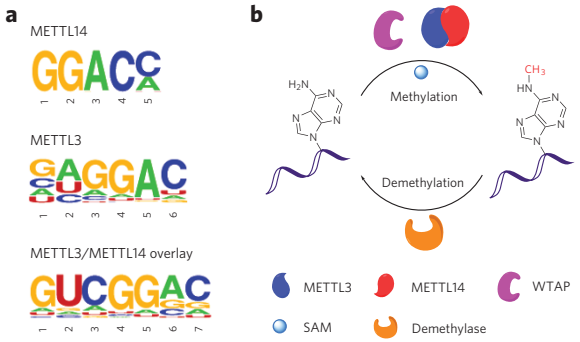

Figure 3 | Identification of RNA-binding sites of METTL3 and METTL14 and a schematic illustration for nuclear RNA *N*^{6}-adenosine methylation. (**a**) Consensus motifs identified within PAR-CLIP–binding sites of METTL3 ($P = 1 \times 10^{-93}$), METTL14 ($P = 1 \times 10^{-47}$) and METTL3–METTL14 overlay ($P = \times 10^{-79}$). (**b**) METTL3 and METTL14 form a heterodimeric methyltransferase complex within the cell nuclei that performs the RNA methylation function. WTAP interacts with the METTL3–METTL14 complex to affect m^{6}A deposition. The demethylase removes the m^{6}A mark, demonstrating a reversible process.

Received 8 November 2013; accepted 2 December 2013; published online 6 December 2013

References

1. Bokar, J.A. in *Fine-Tuning of RNA Functions by Modification and Editing* Vol. 12 (ed. Grosjean, H.), 141–177 (Springer-Verlag, Berlin Heidelberg, 2005).
2. Jia, G., Fu, Y. & He, C. *Trends Genet.* **29**, 108–115 (2013).
3. Motorin, Y. & Helm, M. *Wiley Interdiscip. Rev. RNA* **2**, 611–631 (2011).
4. Beemon, K. & Keith, J.J. *Mol. Biol.* **113**, 165–179 (1977).
5. Jia, G. *et al. Nat. Chem. Biol.* **7**, 885–887 (2011).
6. Zheng, G. *et al. Mol. Cell* **49**, 18–29 (2013).
7. Dominissini, D. *et al. Nature* **485**, 201–206 (2012).
8. Meyer, K.D. *et al. Cell* **149**, 1635–1646 (2012).
9. Bokar, J.A., Shambaugh, M.E., Polayes, D., Matera, A.G. & Rottman, F.M. *RNA* **3**, 1233–1247 (1997).
10. Clancy, M.J., Shambaugh, M.E., Timpte, C.S. & Bokar, J.A. *Nucleic Acids Res.* **30**, 4509–4518 (2002).
11. Hongay, C.F. & Orr-Weaver, T.L. *Proc. Natl. Acad. Sci. USA* **108**, 14855–14860 (2011).
12. Zhong, S. *et al. Plant Cell* **20**, 1278–1288 (2008).
13. Bujnicki, J.M., Feder, M., Radlinska, M. & Blumenthal, R.M.J. *J. Mol. Evol.* **55**, 431–444 (2002).
14. Horiuchi, K. *et al. Proc. Natl. Acad. Sci. USA* **103**, 17278–17283 (2006).
15. Agarwala, S.D., Blitzblau, H.G., Hochwagen, A. & Fink, G.R. *PLoS Genet.* **8**, e1002732 (2012).
16. Bokar, J.A., Rath-Shambaugh, M.E., Ludwiczak, R., Narayan, P. & Rottman, F. *J. Biol. Chem.* **269**, 17697–17704 (1994).
17. Hafner, M. *et al. Cell* **141**, 129–141 (2010).
18. Wang, X. *et al. Nature* doi:10.1038/nature12730 (27 November 2013).
19. Fustin, J.-M. *et al. Cell* **155**, 793–806 (2013).

Acknowledgments

This study was supported by US National Institutes of Health (GM071440 and GM088599). We thank P. Faber and L. Dore for helping with high-throughput sequencing experiments and S.F. Reichard for editing the manuscript.

Author contributions

C.H. conceived the project. J.L. and Y.Y. designed and performed most experiments. D.H. and Z.L. performed high-throughput sequencing data analyses. X.W. and Y.F. helped perform the PAR-CLIP experiment, biochemistry assay and data analysis. L.Z. and M.Y. assisted in expressing recombinant proteins in insect cells. G.J. and W.C. participated in subcloning. X.D. participated in nuclear extract separation. Q.D. synthesized the d_3-m^{6}A standard for LC/MS/MS analysis. J.L., Y.Y. and C.H. wrote the manuscript.

Competing financial interests

The authors declare no competing financial interests.

Additional information

Supplementary information and chemical compound information is available in the online version of the paper. Reprints and permissions information is available online at http://www.nature.com/reprints/index.html. Correspondence and requests for materials should be addressed to C.H.